

**DEVELOPMENT OF BIO-ASH SUPPORTED
NANOCOMPOSITES FOR THE
PHOTOCATALYTIC TREATMENT OF
ACID RED 88 AND METHYLENE BLUE**

LUM PEI TENG

UNIVERSITI SAINS MALAYSIA

2018

**DEVELOPMENT OF BIO-ASH SUPPORTED NANOCOMPOSITES FOR
THE PHOTOCATALYTIC TREATMENT OF
ACID RED 88 AND METHYLENE BLUE**

by

LUM PEI TENG

**Thesis submitted in fulfillment of the
requirements for the degree of
Master of Science**

November 2018

ACKNOWLEDGEMENT

It is with foremost gratitude that I acknowledge to my supervisor Dr. Foo Keng Yuen, who have given his continuous guidance, valuable commentaries, and encouragement as well as his help regarding each experimental work arises throughout the entire study. My sincere appreciation goes to my co-supervisor, Professor Dr. Nor Azazi Zakaria for his supervision on this research work.

Besides, special thanks to all technical and administrative staffs of REDAC centre for their technical assistance in this project. I would like to extent my acknowledgement to the technical staffs of School of Materials and Minerals Resources Engineering USM and School of Chemical Engineering UiTM Permatang Pauh for their assistance on the sample analysis.

Heart-felt gratitude to my parents, and my lovely siblings in providing me their continuous moral support along this research journey. Meanwhile, my special gratitude to my beloved, Moon Wei Chek for his patience, spiritual support and always being with me throughout the toughest process along this study. I am indebted to my friends and team mates for their kindness and assistance.

I would like to convey my deepest appreciation to the financial support provided by the Ministry of Higher Education of Malaysia through the scholarship of MyBrain15. As well, I deeply appreciate those who have directly and indirectly contributed to the accomplishment of this work.

TABLE OF CONTENTS

	Page
ACKNOWLEDGEMENT	ii
TABLE OF CONTENTS	iii
LIST OF TABLES	vii
LIST OF FIGURES	ix
LIST OF PLATES	xii
LIST OF ABBREVIATIONS	xiii
LIST OF SYMBOLS	xvi
ABSTRAK	xvii
ABSTRACT	xix
CHAPTER ONE: INTRODUCTION	
1.1 An overview of the textile waste generation	1
1.2 Problem Statement	3
1.3 Research Objectives	7
1.4 Scope of Study	7
1.5 Significance of study	8
1.6 Organisation of the thesis	9
CHAPTER TWO: LITERATURE REVIEW	
2.1 Textile dyes	11
2.1.1 Characteristics of textile dye effluents	11
2.1.2 Environmental implications of textile dye pollutants	12

2.1.3	Dye treatment technology	14
2.2	Photocatalysis	18
2.2.1	Definition and historical introduction	18
2.2.2	Basic concept and mechanism of photocatalysis	23
2.3	Photocatalysts	25
2.3.1	Semiconductor mediated photocatalysts	25
2.3.1(a)	Zinc oxide	26
2.3.1(b)	Tin (IV) oxide	29
2.3.2	Immobilization of photocatalyst on bio-ash	31
2.4	Evolution of bio-ash derived photocatalysts	33
2.4.1	Properties	33
2.4.2	Preparation techniques and applications on textile dyes degradation	40
2.4.3	Reusability	56
2.5	Summary	57

CHAPTER THREE: MATERIALS AND METHODOLOGY

3.1	Materials and chemicals	58
3.2	Model textile pollutants	61
3.3	Preparation of bio-ash	62
3.3.1	Ashing	62
3.3.2	Acid and base modifications	63
3.4	Preparation of bio-ash supported nanocomposites	63
3.4.1	Preliminary study	63
3.4.2	Preparation procedures	64
3.4.3	Optimization parameter	64

3.5	Photocatalytic reactor	65
3.5.1	Photocatalytic reactor	65
3.5.2	Analytical system	68
3.5.3	Characterization systems	71
3.5.3(a)	Surface morphological analysis	71
3.5.3(b)	Detection of surface functional groups	71
3.5.3(c)	Porosity structure measurement	72
3.5.3(d)	Point of zero charge	72
3.6	Performance evaluation	72
3.7	Batch photocatalytic study	73
3.8	Kinetic study	74
3.9	Reusability test	75
CHAPTER FOUR: RESULTS AND DISCUSSION		
4.1	Synthesis of bio-ash supported nanocomposites	76
4.1.1	Effect of ash impregnation ratio	76
4.2	Physical and chemical characterizations	80
4.2.1	Surface morphology	80
4.2.2	Porosity structure	84
4.2.3	Surface functional groups	88
4.3	Batch photocatalytic study	93
4.3.1	Effect of catalyst loading	93
4.3.3	Effect of solution pH	99
4.3.2	Effect of initial concentration and irradiation time	96
4.4	Kinetic study	103

4.5	Reusability study	110
-----	-------------------	-----

CHAPTER FIVE: CONCLUSION AND RECOMMENDATION

5.1	Conclusion	114
-----	------------	-----

5.2	Recommendation for Future Research	115
-----	------------------------------------	-----

	REFERENCES	118
--	-------------------	-----

APPENDICES

APPENDIX A: Preliminary evaluation of different photocatalysts

APPENDIX B: Historical evolution of photocatalysis

LIST OF PUBLICATIONS AND AWARDS

LIST OF TABLES

	Page
Table 2.1 Typical characteristics of untreated textile effluent at different stages of wet process	12
Table 2.2 Common heavy metals in different classes of industrial textile dyes.	14
Table 2.3 Technical advantages and disadvantages of existing dye treatment technologies.	16
Table 2.4 Physiochemical properties of ZnO.	27
Table 2.5 Physiochemical properties of SnO ₂ .	30
Table 2.6 Brunauer-Emmett-Teller (BET) surface area and total pore volume of different ash based photocatalytic composites.	38
Table 2.7 A comprehensive summary of the bio-ash supported nanocomposites.	45
Table 2.8 Application of bio-ash derived nanocomposites for the photodegradation of textile dyes.	51
Table 3.1 Initial raw precursors applied in this work.	59
Table 3.2 List of chemicals and reagents.	60
Table 3.3 List of apparatus and instruments.	61
Table 3.4 Structural and molecular properties of Acid Red 88 and Methylene Blue.	62
Table 3.5 Preparation parameters for the synthesis of bio-ash supported nanocomposites.	65
Table 3.6 Experimental parameters and the corresponding ranges for the photodegradation process.	74
Table 4.1 Surface physical characteristics of raw IA, DSA and CA.	86
Table 4.2 Surface physical characteristics of SnO ₂ /IA, SnO ₂ /DSA and SnO ₂ /CA.	87
Table 4.3 Surface physical characteristics of ZnO/IA, ZnO/DSA and ZnO/CA.	88

Table 4.4	Point of zero charge (pH_{zpc}) of the SnO ₂ derived nanocomposites.	101
Table 4.5	Point of zero charge (pH_{zpc}) of the ZnO derived nanocomposites.	102
Table 4.6	The apparent kinetic rate constants for the photodegradation of AR 88 at different initial concentrations.	106
Table 4.7	The apparent rate kinetic constants for the photodegradation of MB at different initial concentrations.	106
Table 4.8	A comparison of the photocatalytic performance of different photocatalysts for the degradation of AR 88 and MB.	107
Table 4.9	A comparison of the photocatalytic performance of different regenerated photocatalysts for the photocatalytic degradation of dye pollutants.	113

LIST OF FIGURES

	Page
Figure 2.1	Dye treatment technology. 15
Figure 2.2	Number of publications related to photocatalysis from 2013-2017 in different countries. 18
Figure 2.3	Historical timeline of photocatalysis from 1910s to 2010s. 19
Figure 2.4	Schematic diagram of the electrochemical photocell. 22
Figure 2.5	Schematic diagram of basic photocatalytic processes over photon activated semiconductor photocatalyst. 23
Figure 2.6	Crystal structure of ZnO in (a) cubic rocksalt, (b) cubic zinc blende and (c) hexagonal wurtzite. 26
Figure 2.7	Different morphologies of ZnO in nanoparticles, nanosheets, nanoflowers, nanorods, nanocombs and nanowires. 28
Figure 2.8	Rutile structure of SnO ₂ . 30
Figure 2.9	Surface morphology of SnO ₂ nanoparticles. 31
Figure 2.10	Scanning Electron Micrographs (SEM) of raw (a) RHA, (b) FA and (c) VA. 34
Figure 2.11	Scanning Electron Micrographs (SEM) of (a) TiO ₂ -RHA, (b) TiO ₂ -FA and (c) TiO ₂ -VA. 35
Figure 2.12	Fourier Transform Infra-red Spectroscopy (FTIR) of (a) FA based composite and (b) RHA based composite. 37
Figure 2.13	Nitrogen adsorption-desorption curves of the (a) FA based composite and (b) RHA based composite. 40
Figure 3.1	Flowchart of research activities. 59
Figure 3.2	Measurement principles of (a) solid and (b) solution samples. 69
Figure 3.3	The standard calibration curves for (a) AR 88 and (b) MB. 70
Figure 4.1	Effect of ash impregnation ratio on the SnO ₂ derived nanocomposites for the photodegradation of AR 88 (catalyst loading = 0.01 g/100 mL; C ₀ = 500 mg/L; t = 30 min). 77

Figure 4.2	Effect of ash impregnation ratio on the ZnO derived nanocomposites for the photodegradation of MB (catalyst loading = 0.10 g/100 mL; $C_0 = 200$ mg/L; $t = 60$ min).	77
Figure 4.3	Schematic diagram of the bio-ash derived nanocomposites at the (a) optimum impregnation ratio and (b) beyond the optimal impregnation ratio.	79
Figure 4.4	Nitrogen adsorption-desorption curve of (a) SnO ₂ /IA, (b) SnO ₂ /DSA, (c) SnO ₂ /CA (d) ZnO/IA, (e) ZnO/DSA, and (f) ZnO/CA derived nanocomposites.	85
Figure 4.5	Fourier-Transform Infrared spectra of (a) IA, and (b) ZnO/IA and (c) SnO ₂ /IA derived nanocomposites.	90
Figure 4.6	Fourier-Transform Infrared spectra of (a) DSA, and (b) ZnO/DSA and (c) SnO ₂ /DSA derived nanocomposites.	91
Figure 4.7	Fourier-Transform Infrared spectra of (a) CA, and (b) ZnO/CA and (c) SnO ₂ /CA derived nanocomposites.	92
Figure 4.8	Effect of catalyst loading on the photodegradation of AR 88 ($C_0 = 500$ mg/L; $t = 30$ min).	95
Figure 4.9	Effect of catalyst loading on the photodegradation of MB ($C_0 = 200$ mg/L, $t = 60$ min).	95
Figure 4.10	Plot of degradation of AR 88 as a function of initial concentrations and irradiation time by (a) SnO ₂ /IA, (b) SnO ₂ /DSA and (c) SnO ₂ /CA.	97
Figure 4.11	Plot of degradation of MB as a function of initial concentrations and irradiation time by (a) ZnO/IA, (b) ZnO/DSA and (c) ZnO/CA.	98
Figure 4.12	Effect of solution pH on the photodegradation of AR 88 ($C_0 = 500$ mg/L; $t = 30$ min).	100
Figure 4.13	Effect of solution pH on the photodegradation of MB ($C_0 = 200$ mg/L; $t = 60$ min).	102
Figure 4.14	Plots of kinetic study for the photodegradation of AR 88 at different initial concentrations by (a) SnO ₂ /IA, (b) SnO ₂ /DSA and (c) SnO ₂ /CA.	104
Figure 4.15	Plots of kinetic study for the photodegradation of MB at different initial concentrations by (a) ZnO/IA, (b) ZnO/DSA and (c) ZnO/CA.	105

Figure 4.16 Reusability test of bio-ash supported nanocomposites for the 111
photodegradation of (a) AR 88 and (b) MB ($C_0 = 100$ mg/L; $t =$
30 min).

LIST OF PLATES

		Page
Plate 3.1	Exterior view of self-assembled photocatalytic reactor (a) without operation and (b) during operation.	66
Plate 3.2	Interior view of self-assembled photocatalytic reactor (a) without operation and (b) during operation.	67
Plate 4.1	Scanning electron micrographs of raw (a) IA, (b) DSA and (c) CA.	81
Plate 4.2	Scanning electron micrographs of (a) SnO ₂ /IA, (b) SnO ₂ /DSA and (c) SnO ₂ /CA derived nanocomposites.	82
Plate 4.3	Scanning electron micrographs of (a) ZnO, and (b) ZnO/IA, (c) ZnO/DSA and (d) ZnO/CA derived nanocomposites.	84

LIST OF ABBREVIATIONS

AC	Activated carbon
A-FA	Amine functionalized fly ash
AOP	Advanced oxidation process
AR 1	Acid Red 1
AR 88	Acid Red 88
BB	Bermacid Blau
BCA	Bone char ash
BET	Brunauer-Emmett-Teller
BOD ₅	Biochemical oxygen demand
BR	Bermacid Rot
BSE	Backscattered electron
CA	Coffee residue ash
CB	Conduction band
CFA	Coal fly ash
CTAB	Cetyltrimethylammonium bromide
COD	Chemical oxygen demand
Cts	Chitosan
CuPc	Copper phthalocyanine complex
DSA	Durian shell ash
FA	Coal fly ash
FAC	Fly ash cenosphere
FAG	Fly ash based geopolymer
FAP	Fly ash particle

FAZ-X	Fly ash-derived zeolite X
FMS	Fly ash bead
FT-IR	Fourier-Transform Infrared
GBAG	Grapheme bottom ash geo-polymeric
GR	Graphene
HTAB	Hexadecyltrimethylammonium bromide
IA	Incense ash
IUPAC	International Union of Pure and Applied Chemistry
LBLA	Layer-by-layer assembly
LFA	Lignite fly ash
MCM-48	Mobil Composition of Matter-48
MFAC	Magnetic fly ash cenosphere
MO	Methyl Orange
MOD	Modified metalorganic decomposition
MB	Methylene Blue
PEC	Photoelectrochemical
PEG	Polyethylene glycol
PL	Photoluminescence
PVP	Polyvinylpyrrolidone
RB 5	Reactive Black 5
RHA	Rice husk ash
Rh B	Rhodamine-B
RO 4	Reactive Orange 4
RSA	Rice straw ash
SE	Secondary electron

SEM	Scanning Electron Microscopy
SS	Suspended solid
TB	Tryphan Blue
TOC	Total organic carbon
TSS	Total suspended solid
TVA	Ti-containing volcanic ash
UV	Ultraviolet
UV-Vis	Ultraviolet-visible
VA	Volcanic ash
VB	Valence band
Zeo	Zeolite

LIST OF SYMBOLS

ΔE	Band gap energy
λ	Wavelength
ε	Absorption coefficient
Abs	Absorbance
a	Lattice constant a
c	Lattice constant c
C	Concentration
C_0	Initial concentration
C_t	Concentration at time t
e_{CB}^-	Electron in the conduction band
$h\nu$	Photon energy
h_{VB}^+	Positive hole in valence band
I_0	Intensity of light without the sample set
I_t	Intensity of light incident upon sample cell
K_{app}	Apparent pseudo-first order kinetic rate constant
L	Cell's optical path length
P/P_0	Relative pressure
$pH_{initial}$	Initial pH
pH_{final}	Final pH
pH_{zpc}	Point of zero charge
R^2	Determination coefficient
T	Transmittance
t	Reaction time

**PENYEDIAAN KOMPOSIT NANO BERASASKAN ABU-BIO UNTUK
PERAWATAN PEWARNA MERAH ASID 88 DAN BIRU METILENA
SECARA PEMANGKINAN FOTO**

ABSTRAK

Setakat ini, applikasi pemangkinan foto secara skala besar, satu teknologi baru yang inovatif bagi pemulihan alam sekitar daripada bahan pencemar pewarna tekstil, sedang mengalami cabaran teknikal zarah-aglomerasi diri dan kesukaran perpisahan selepas proses perawatan. Penyelidikan tentang imobilisasi pemangkin foto pada bahan sokongan yang berbeza telah dipromosikan. Dengan memandangkan peningkatan kuantiti dan menonjolkan nilai ekonomi abu-bio yang rendah, penyediaan satu siri komposit nano pemangkinan foto berasaskan abu-bio melalui teknik salutan fizikal dan kaedah hidro-haba telah dicuba. Abu-bio termasuk abu kemenyan (IA), abu kulit durian (DSA) dan abu sisa kopi (CA) telah digunakan sebagai prekursor kos rendah untuk penyediaan komposit nano SnO₂ dan ZnO berasaskan abu-bio, dengan nisbah jerap abu yang berbeza dari 1:1 ke 1:5. Analisis morfologi permukaan, pengukuran struktur liang, pengesanan kumpulan fungsi permukaan dan penilaian titik capaian arus sifar (pH_{zpc}) telah dikendalikan. Prestasi komposit nano pemangkinan foto yang disediakan diuji dengan degradasi foto bagi pewarna merah asid (AR 88) dan biru metilena (MB), dengan perubahan parameter operasi yang berbeza, termasuk dos pemangkin, kepekatan asal pewarna dan masa penyinaran, serta pH larutan. Kajian morfologi permukaan menunjukkan pemendapan nanopartikel pemangkin pada permukaan abu-bio yang berbeza telah berjaya dicapai. Pemeriksaan perkembangan keliangan mencadangkan kebolehan abu-bio dalam meningkatkan sifat permukaan

komposit nano secara keseluruhannya. Spektrum Fourier-Transform Infrared Spektroskopi menandakan pemendapan seragam pemangkin SnO₂ dan ZnO pada permukaan menandakan abu-bio. Hasil kajian ini menunjukkan keberkesanan degradasi foto dicapai dengan dos pemangkin optimum, pada 0.03 g/100 mL bagi komposit nano SnO₂/CA, 0.04 g/100 mL bagi komposit nano SnO₂/IA dan SnO₂/DSA, dan 0.40 g/100 mL bagi komposit nano ZnO/IA, ZnO/DSA dan ZnO/CA, masing-masing. Peningkatan kepekatan asal AR 88 dari 100-500 mg/L dan MB dari 50-400 mg/L menyaksikan kesan yang nyata terhadap pengurangan kecekapan penyingkiran, dan memerlukan masa penyinaran yang lebih panjang untuk proses penyingkiran yang sempurna. Medium asid sesuai untuk penyingkiran foto bagi AR 88, manakala keadaan alkali lebih sesuai untuk degradasi foto bagi MB. Analisis kinetik memperlihatkan bahawa model kinetic untuk degradasi foto sesuai dipadankan dengan persamaan model pertama. Ujian penggunaan semula menandakan ketahanan komposit nano baru yang tinggi, dengan kecekapan degradasi foto yang melebihi 85% walaupun selepas lima kitaran penggunaannya. Kajian ini menzahirkan pandangan baru dalam penyediaan komposit nano abu-bio kos rendah dan mesra alam untuk perawatan berkesan pencemar tekstil.

**DEVELOPMENT OF BIO-ASH SUPPORTED NANOCOMPOSITES FOR
THE PHOTOCATALYTIC TREATMENT OF ACID RED 88 AND
METHYLENE BLUE**

ABSTRACT

To date, the wide scale application of photocatalysis, a new innovative and promising technology for the environmental remediation of textile dye pollutants, is experiencing the technical challenges of particles self-agglomeration and post-separation difficulty. Arising research pertaining to the immobilization of photocatalysts onto different supporting materials have been promoted. Giving insight into the huge generation of agricultural bio-ash and highlighting of their low economical value, the development of a series of bio-ash supported nanocomposites by using simple physical coating and hydrothermal techniques has been attempted. Bio-ash including incense ash (IA), durian shell ash (DSA) and coffee residue ash (CA) was adopted to be the low-cost precursors for the preparation of bio-ash supported SnO₂ and ZnO nanocomposites, with different ash impregnation ratio from 1:1 to 1:5. Surface morphology analysis, pore structural measurement, detection of surface functional groups and evaluation of point of zero charge (pH_{zpc}) were carried out. The photocatalytic performance was examined with respect to the batch photocatalytic degradation of Acid Red 88 (AR 88) and Methylene Blue (MB) by varying the operational parameters, catalyst loading, initial dye concentration and irradiation time, and solution pH. Surface morphological studies revealed that the deposition of catalysts onto the surface of different bio-ash was successfully attained. Examination of the porosity development suggested that the capability of bio-ash to improve the overall surface area. Fourier-Transform Infrared

Spectroscopy (FT-IR) spectrum ascertained the homogenous deposition of SnO₂ and ZnO photocatalysts on the surface of bio-ash. Results illustrated the best photodegradation efficacy was achieved at the optimum catalyst loading of 0.03 g/100 mL for SnO₂/CA, 0.04 g/100 mL for SnO₂/IA and SnO₂/DSA nanocomposites, and 0.40 g/100 mL for ZnO/IA, ZnO/DSA, and ZnO/CA nanocomposites, respectively. Acidic medium favors to the photocatalytic removal of AR 88, while the basic condition prefers to the photodegradation of MB. Increasing initial concentration from 100-500 mg/L for AR 88 and from 50-400 mg/L for MB demonstrated the significant influences on the removal efficacy, and a longer irradiation time was acquired for the complete removal process. Kinetic analysis revealed that the linearity of the photocatalytic plots was well described by the first order model. Reusability test indicated high durability of these newly prepared nanocomposites, with greater than 85% of degradation efficiency even after five regeneration cycles. This study provided a new insight in the preparation of valuable bio-ash supported nanocomposites for the effective purification of textile dye pollutants.

CHAPTER ONE

INTRODUCTION

1.1 An overview of the textile waste generation

Production of textile fibre is one of the largest water-consuming industries in the world. The water is mainly used for application of chemicals onto the fibres and rinsing of the manufactured textiles. A large amount with about 0.08-0.15 m³ of water is used to produce 1 kg of fabrics, notably in wet treatment process, and an estimation of about 1000-3000 m³ of wastewater is generated after the processing of about 12-20 tonnes of textiles per day (Ghaly *et al.*, 2014). These untreated textile effluents contain large amount of dyes, chemicals, organic and inorganic compounds containing trace metals including Cr, As, Cu and Zn, which are capable of detrimental to the environment and human health. Extensive application of dyes in dyeing and finishing process are the major sources of industrial effluents pollution. The usage of dyes varies from industry to industry, and the application of dyes primarily depends on the types of fabrics manufactured. There are three different types of fabrics used in the manufacture of various textile products, including cellulose fibres (cotton, rayon, linen, ramie, hemp and lyocell), protein fibres (wool, angora, mohair, cashmere and silk) and synthetic fibres (polyester, nylon, spandex, acetate, acrylic, ingeo and polypropylene). Reactive dyes, direct dyes, naphthol dyes and indigo dyes are commonly applied to dye cellulose fibres. Protein fibres are dyed using azo dyes and lanaset dyes. Dispersed dyes, basic dyes and direct dyes are applied for the dyeing of synthetic fibres (Chequer *et al.*, 2013).

During the dyeing and finishing processes, there is always a portion of these dyes that remains unfixed to the fabrics, due to their incomplete exhaustion and dye hydrolysis in the alkaline dye bath and released into the environment. These unfixed dyes are found to be in high concentrations in textile effluents (Suresh, 2014). Among all, there are exceeding 100,000 types of commercially available dyes, and it is predicted that 90% of them would end up in fabrics, while the remaining portion is applied in leather, paper, plastic, and chemical industries (Vinu and Madras, 2009).

Malaysia has been recognized as the ninth largest producer of textile fibres in Asian regions in 2012, which has contributed more than 1.8% to the total exports of manufactured goods in Malaysia (MIDA, 2018). There are more than 970 licensed textile factories in Malaysia. Several textile products including natural or man-made fibres, woven or non-woven fabrics, knitted fabrics, specialized apparel, technical and functional textile have been introduced as promoted textile products under the Promotion of Investment Act, 1986 (MIDA, 2018). Amongst all, man-made fibres such as nylon, polyester filament, and staple are the most dominant textile products that contribute to the most economic growth of Malaysia, particularly in the states of Terengganu and Kelantan, East Coast of Peninsular Malaysia (Pang and Abdullah, 2013). Meanwhile, the rising water pollution problem triggered by the dye usage in finishing step of the textile industries, accounting for more than 22% of the total industrial wastewater generation, recorded the highest volume in Johor (28.6%), Penang (28.2%) and Selangor (15.6%).

In guarding the environment from pollution caused by the textile industry, several environment protection agencies worldwide have imposed certain standard limits on the disposal of effluents into the environment. The disposal limits are found to differ from country to country. In Malaysia, the discharge quality standards are

stipulated in the environmental quality (sewage industrial effluent) regulations, 2009, to comply with the minimum requirements of the Environmental Quality Act 1974 (DOE, 2010), classified as standards A (discharged upstream) and B (discharged downstream) based on the location of the industrial area. The current colour unit used in Malaysia is American Dye Manufacturers Institute (ADMI) colour, that based on the spectrophotometric method. Accordingly, the maximum effluent parameter limits of coloured dyes are 100 ADMI for standard A and 200 ADMI for standard B (DOE, 2010). Since the presence of dyes in textile industrial effluent is highly undesirable, numerous treatment techniques ranging from physical, chemical and biological approaches have been developed for the possible remediation of different multi-components pollutants in wastewater to meet the legislative requirement.

1.2 Problem Statement

Textile effluent is a cause of significant amount of environmental degradation and human illnesses. A developing research adopting different treatment techniques, notably flocculation, coagulation, membrane filtration, ion-exchange and adsorption have gained a promising level of success. However, these individual treatment processes are featured by the limitations associated with the pollutants phase transfer, which would trigger to the release of secondary pollutants to the environment and additional post-treatment of the sludge disposal is deeply required (Affam *et al.*, 2016). Meanwhile, the presence of one or several benzene rings in the dye structure could render these treatment process to be ineffective in degrading the organic pollutants. Although, biological treatment techniques such as aerobic and anaerobic process are being applied in textile industry by using different kind of microorganisms (Ghaly *et*

al., 2014). Nevertheless, the application is restricted by the presence of toxic heavy metals in the effluent that might affect the growth of microorganism, with longer time is needed for the complete degradation process. Furthermore, most of the dyes released in textile effluents are non-biodegradable in nature. Hence, advanced oxidation processes (AOPs), notably photocatalysis have gained much attention from researchers owing to efficiency and ability to treat almost all solid components in textile effluents.

Semiconductor-mediated photocatalysis, also known as heterogeneous photocatalysis is recognized as one of the best “green” technology to confront with the challenges of environmental pollutions, owing to the excellent photocatalytic decomposition capacity to completely mineralize a variety of noxious pollutants, and free from the generation of secondary pollutants (Madhavan *et al.*, 2009). Semiconductor metal oxides, primarily titanium dioxide (TiO₂), zinc oxide (ZnO), bismuth vanadate (BiVO₄), tungsten oxide (WO₃), ceric dioxide (CeO₂) and tin dioxide (SnO₂) with different band gap energies and solar energy transformation, have been applied extensively as promising photocatalysts for water treatment process (Lu *et al.*, 2013). Notwithstanding the distinctive properties, the direct application of semiconductor metal oxides is still experiencing a series of technical challenges towards its practicality pertaining to their low stability, and lower degradation efficiency, which the particles self-agglomeration and post-separation difficulty remain a major problem.

Among all, the most commonly used photocatalyst, TiO₂ possess poor quantum yield due to the rapid recombination of photogenerated electron-hole pairs, poor and selective adsorption, low surface area, and short-lived photo-generated carriers, would hinder the efficiency of photodegradation reaction (Zhang *et al.*, 2014c;

Zhu *et al.*, 2016). The broad band gap energy of SnO₂, as similar as TiO₂, would restrict their applications under visible light, due to the reason that ultraviolet (UV) light accounts only for a small fraction, with merely 4% as compared to the visible light (Lv *et al.*, 2013). Similarly, ZnO with poor adsorption capacity, owing to the non-porous structure, could suppress its performance in the photocatalytic reaction. Additionally, it is unstable either in highly acidic or alkaline conditions, and rapid deactivated in bulk due to the high tendency of self-aggregation (Ökte and Karamanis, 2013). The fine nanoparticle size of the catalyst powder together with their surface energy, would generate a strong tendency to the catalyst self-agglomeration during the operation. Besides, ZnO is found to be highly detrimental in views of the surface-area reduction and low reusable lifespan correspond with post-separation difficulty after it serves its purposes in water treatment process (Chong *et al.*, 2010).

Consequently, most of the practical application and system design of commercial photocatalysts are mainly deteriorated by the enormous perpetual fatal limitation associated with the difficulty of recovery, and additional separation process is required for their regeneration from the system. In an effort towards overcoming the aforementioned drawbacks, arising researches have been conducted to immobilize the catalyst onto different supporting materials. Accordingly, the immobilization of new supporting materials to the photocatalysts: alumina (Sepehri *et al.*, 2016), silica (Karimi *et al.*, 2016), glass (Jia *et al.*, 2016), clay (Hadjltaief *et al.*, 2016), graphite (Prabakar *et al.*, 2016), activated carbon (Pan *et al.*, 2016) and zeolite (Derikvandi and Nezamzadeh-Ejhieh, 2017b) have been examined. Lately, attention has been drawn to the innovative utilization of aesthetic biomass derived ash as the major resources of the possible supporting surface for the production of high-quality photocatalysts.

Statistical data has illustrated that the worldwide generation of agricultural waste is approximately 998 million tonnes per year and in Malaysia, an estimation of 1.2 million tonnes of agricultural biomass is produced annually (Agamuthu, 2009; Obi *et al.*, 2016). Simple act of burning agricultural waste as energy and fuel is one of the oldest biomass conversion processes and is still the dominant technology accounting for more than 95% of all biomass energy utilized today (Obi *et al.*, 2016). Upon the combustion process, the burning by-product, about 476 million tonnes of bio-ash was generated per year (Vassilev *et al.*, 2010). These hugely generated bio-ash, which are commonly applied as low-economical value end-products, have been investigated to be the low-cost catalyst supports owing to the great potential of these bio-ash as a novel adsorbent, with significant specific surface area, high adsorption capability, ion-exchange capacity and unique reusability (Vassilev *et al.*, 2013b). These features are mainly ascribed to the presence of the alkali and alkaline earth oxides, (Vassilev *et al.*, 2010), specifically oxygen-containing groups, calcite and quartz to induce a negative charge on the surface of ash in the alkaline aqueous phase, which make them available for positive charged metal ions adsorption (Srivastava *et al.*, 2006).

The present available studies have been limited on the application of rice husk ash (Adam *et al.*, 2013), volcanic ash (Borges *et al.*, 2008) and coal fly ash (Surolia *et al.*, 2010) as the catalyst supports, while there are still a paucity of researches on the utilization of bio-ash as the renewable supporting materials. Therefore, this study was conducted to develop a series of valuable photocatalysts by using bio-ash as the catalyst supports for the photocatalytic treatment of dye pollutants.

1.3 Research Objectives

The principal objective of this study is to synthesize a series of bio-ash supported nanocomposites for the photocatalytic treatment of Acid Red 88 and Methylene Blue. The present study aims at the following objectives:

- a. To characterize the physical and chemical properties of the photocatalytic nanocomposites in terms of the surface morphology, surface functional groups, and porosity structure.
- b. To optimize the performance for the photocatalytic treatment of Acid Red 88 and Methylene Blue, in the variation of catalyst loading, initial concentration and irradiation time, and solution pH.
- c. To establish the kinetic of the photocatalytic degradation of Acid Red 88 and Methylene Blue.
- d. To examine the reusability of the newly prepared bio-ash supported nanocomposites.

1.4 Scope of Study

The present study highlighted the novel application of bio-ash as the renewable supporting materials for the synthesis of photocatalytic nanocomposites, mainly incense ash (IA), durian shell ash (DSA) and coffee residue ash (CA). The simple physical mixing method and one step hydrothermal technique have been adopted as the unique catalyst preparation procedure. The changing metal oxide/ash impregnation ratio to the photocatalytic performance was optimized.

These newly synthesized nanocomposites were subjected to the evaluation of surface morphology by Scanning Electron Microscopy (SEM), porosity structure by nitrogen adsorption–desorption isotherm, surface functional groups by Fourier Transform Infrared (FTIR) Spectroscopy and the determination of the point of zero charge (pH_{zpc}). Performance analysis was carried out by varying the operational parameters, including the catalyst loading, initial concentration and irradiation time, and solution pH for the photocatalytic degradation of AR 88 and MB. Kinetic analysis was performed according to the pseudo-first order kinetic model, while the stability of these newly prepared nanocomposites was assessed by using the reusability test of up to five successive regeneration cycles.

1.5 Significance of study

To date, a new evolution of the development of ideal photocatalysts by using several unique approaches, including dye sensitization (Altm *et al.*, 2016), semiconductor coupling (Derikvandi and Nezamzadeh-Ejhieh, 2017a), doping (metal and non-metal doping) (Hasché *et al.*, 2016) and photocatalyst immobilization (Lin *et al.*, 2017) have been widely explored. Accordingly, the research pertaining to the immobilization of new supporting materials to the photocatalysts, such as biomass derived ash with the extensively highlighted problem related to the combustion of biomass by a huge number of industrial development projects was conducted.

This study implemented the concept of “waste to wealth” strategy, to propose the renewable utilization of bio-ash as the secondary resources for the preparation of eco-friendly photocatalytic nanocomposites, with its unique favorable properties: low cost, non-toxicity, lightweight, and physical and chemical stability. This novel

approach would promote the preparation of natural supporting surface from bio-ash, an abundantly available, non-toxic and low-cost resource, contributing to the environmental sustainability. Technological enhancement in this area, as well as knowledge enhancement related to the advocacy of waste conversion strategy, could be further developed, and turn into a new intellectual property and water treatment technique.

The innovation also supports the implementation of Malaysia Green Technology Master Plan, with the major framework to achieve 40% of carbon intensity reduction through the launching of Green Catalyst Projects (GCP), and in according to Sustainable Development Goals (SDGs), specifically goal 6 (Clean Water and Sanitation) in terms of encouraging the efficiency of water treatment technologies to protect and restore water-related ecosystem.

1.6 Organisation of the thesis

This thesis is structured into five major chapters. Chapter One outlined an overview of the textile waste generation. The problem associated with the major needs of advanced treatment technology and bio-ash supported photocatalysts, research objectives, scope of the study, significance or major contributions of this work were elucidated. Chapter Two provided the literature finding related to the characteristic of textile dye effluents, environmental implications, and treatment technologies. The definition, historical background, and fundamental knowledge of photocatalysis were highlighted. Additionally, a comprehensive review on the bio-ash and bio-ash supported photocatalytic nanocomposites were underlined.

Chapter Three summarized the catalyst preparation process, characterization techniques, as well as performance evaluation, kinetic studies and reusability assessment of the photocatalytic nanocomposites. A step-wise description of the experimental reactor setup and a summary of the research activities were presented. Chapter Four outlined the major findings throughout this research. Discussions related to the results were elucidated from the perspective of preparation parameters, physical and chemical characteristics of the newly bio-ash derived photocatalysts, performance evaluation, optimized experimental conditions, kinetic test and reusability potential. This chapter was ended with the comparison of the crucial findings from the present study with other relevant researches. Chapter Five summarized the critical findings from this study related to the research objective. Further recommendations and considerations for the future studies were proposed.

CHAPTER TWO

LITERATURE REVIEW

This chapter provides a comprehensive literature pertaining to the background information of textile dyes, including the characteristic, environmental implications and the treatment technologies for textile effluents. The (1) definition and historical development, (2) basic mechanism of photocatalysis, (3) semiconductor mediated photocatalyst and (4) immobilization of photocatalyst are highlighted. The fundamental knowledge of bio-ash, and up-to-date information related to the bio-ash derived photocatalysts, in terms of their unique properties, preparation techniques, relevant application for the textile dye removal as well as their reusability are deeply elucidated.

2.1 Textile dyes

2.1.1 Characteristics of textile dye effluents

The characteristics of textile dye effluents may vary and depended on the type of textile manufactured and the chemicals applied. Generally, these untreated textile wastewater effluents are high in suspended solids (SS) and dissolved solids content, biological oxygen demand (BOD₅), chemical oxygen demand (COD), pH, temperature, odour, turbidity, toxicity and colour. Specifically, most of the BOD₅/COD ratios are found to be around 1:4, indicating the presence of non-biodegradable substances (Ulucan-Altuntas and Ilhan, 2018). The typical characteristics of untreated textile effluent at various stages of the wet process are given in Table 2.1. These textile effluents contain a number of trace metals such as Cr, As, Cu and Zn, which are

capable of harming the environment. The suspended solids (SS) may interfere the oxygen transfer mechanism in the air-water interface, while the presence of inorganic substances, in the form of hydrochloric acid, sodium hypochlorite, sodium hydroxide and sodium sulphide even at a lower concentration are found to be toxic to aquatic life (Ghaly *et al.*, 2014).

Table 2.1: Typical characteristics of untreated textile effluent at different stages of wet process (Ghaly *et al.*, 2014; Pang and Abdullah, 2013).

Processes	Characteristic
Fiber manufacturing	High BOD ₅ , COD, medium SS
Spinning and weaving	High BOD ₅ , COD, SS
Desizing	Very small volume, high BOD ₅ (30-50% of total)
Scouring	Very small, strongly alkaline, dark colour, high BOD ₅ values (30% of total), high pH, 70-80 °C
Bleaching	Small volume, strongly alkali, low BOD ₅ (5% of total), high pH
Mercerizing	Small volume, strongly alkaline, low BOD ₅ (less than 1% of total), high pH, SS
Dyeing	Large volume, strongly coloured, fairly high BOD ₅ (6% of total), high pH, SS
Printing	Very small volume, oily appearances, fairly high BOD ₅ , high pH, SS, strong colour
Finishing	Low alkalinity, low BOD ₅ , traces of starch, tallow, salts, special finishes

2.1.2 Environmental implications of textile dye pollutants

Today, water pollution related to the emission of textile dyes, remains an emerging environmental problem among the scientific community. The discharge of

these dye contaminated effluents into the natural water resources is undesirable, due to the persistent dyes and their breakdown intermediate products, which are hazardous and detrimental to the environment. Owing to the high tinctorial value of less than a ppm of dye in water, that could produce highly coloured elements, besides giving rise to the aesthetic issue, this phenomenon has significantly affected the photosynthetic function of aquatic plants (Akpan and Hameed, 2009; Gupta *et al.*, 2003), by blocking the sunlight from penetrating through water and reducing the capacity of marine plant in food production (Holkar *et al.*, 2016; Koswojo *et al.*, 2010). Dye pollutants also increase the BOD₅ of the receiving water, in turn reduce the reoxygenation process and hence hamper the growth of photoautotrophic organisms, by threatening the equilibrium of the food chain (Holkar *et al.*, 2016).

The presence of metals in different dyes is essential for their role as textile colorants. Table 2.2 shows heavy metal content including copper, chromium, lead, manganese, cadmium, nickel, and zinc in different dye classes (Verma, 2008). The release of these metals and the persistent dyes structure with toxicity properties might cause negative impacts on natural ecosystems or even hazardous to human health. These recalcitrant dyes with the presence of carcinogens, including benzidine, naphthalene and other aromatic intermediate compounds, are claimed to be toxic, carcinogenic, genotoxic, teratogenic and mutagenic that might affect the flora, fauna and human health in a long-term exposure (Suteu *et al.*, 2011). For instance, triphenylmethane dyes such as crystal violet and acid violet are phytotoxicity to plants, cytotoxic to mammalian cells and possible to cause a tumour growth in some species of fish (Jadhav *et al.*, 2012).

Table 2.2: Common heavy metals in different classes of industrial textile dyes (Verma, 2008).

Dye classes	Heavy metals content
Acid dyes	Copper, lead, zinc, chromium, cobalt
Basic dyes	Copper, lead, zinc, chromium
Direct dyes	Copper, lead, zinc, chromium
Mordant dyes	Chromium
Pre-metallized dyes	Cobalt, chromium, copper
Reactive dyes	Copper, chromium, lead
Vat dyes	None
Disperse dyes	None

Additionally, prolonged human exposure to these textile dyes are capable to induce skin and eyes abnormality, irritation of respiratory and gastrointestinal tracts, asthma, allergic contact dermatitis or nasal problems (Merouani *et al.*, 2010). The stable structure and non-biodegradable nature of these persistent dyes remain a great challenge. Hence, it is pertinent and ecologically noteworthy to the evolution of a novel and effective textile wastewater treatment technique.

2.1.3 Dye treatment technology

Dyes are considered as an objectionable kind of contaminants due to their hazardous impacts to the environment and human health. As such, it is essential to treat the coloured textile effluents effectively by using various non-destructive and destructive dye removal techniques as stated in Figure 2.1.

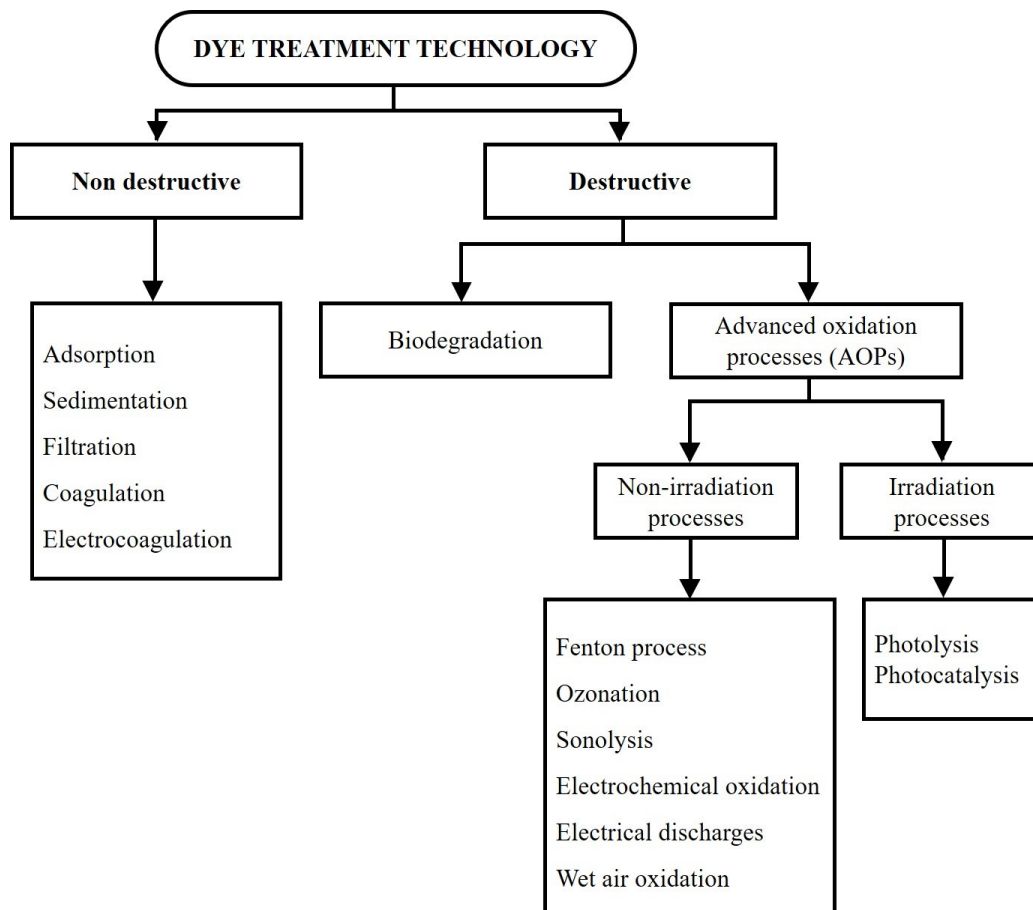


Figure 2.1: Dye treatment technology (Fernández *et al.*, 2010).

Non-destructive techniques are commonly applied, owing to the primary advantage of efficient in most cases, and applicable for all types of dyes. During the application, these dyes could be transferred into other phases, which require further post-treatment, due to the generation of new secondary waste after the treatment process. Typically, the dye treatment methodologies are deeply classified into three categories: (a) physical, (b) chemical, and (c) biological treatment (Pang and Abdullah, 2013), including filtration, coagulation-flocculation, adsorption, biodegradation and advanced oxidation processes (AOPs) (Fenton process, ozonation, electrochemical oxidation, sonolysis, and photocatalysis) as given in Table 2.3.

Photocatalysis is one of the series of AOPs that involves the generation of highly reactive hydroxyl radicals through the excitation of electrons, by the activation

of a light source, to decompose various type of dyes (Gupta and Suhas, 2009). The advantage of photocatalytic treatment is the potential of mineralization of dyes within a relatively short reaction time without the production of sludge. The main drawbacks of this process are the limitations of fine catalyst post-separation and the fouling of catalyst. Today, numerous studies have been initiated to immobilize the catalyst with the new supporting materials to overcome the limitations associated with the post-separation. Owing to its high degradation efficiency, photocatalysis could be a promising alternative solution for the possible treatment of dye contaminants.

Table 2.3: Technical advantages and disadvantages of existing dye treatment technologies.

Dye removal techniques	Advantages	Disadvantages
Filtration technology	<p>(a) No chemicals use and simple automation for ultrafiltration.</p> <p>(b) Applicable for diverse range of dye waste, relatively insensitive to flow and simple operation for reverse osmosis.</p>	<p>(a) High working pressure, high cost of membrane, significant energy consumption and a relatively short life of membrane make their use limited for dye removal.</p> <p>(b) Frequent cleaning and replacement of the modules to maintain the effectiveness are required.</p>
Coagulation-flocculation	<p>(a) Economically feasible with satisfactory removal of disperse, vat and Sulphur dyes.</p>	<p>(a) The major drawbacks of this process are high cost of coagulating agent, and excessive use of chemicals and the pollutant removal process is pH dependent.</p>

Table 2.3: Continued.

Dye removal techniques	Advantages	Disadvantages
Coagulation-flocculation		(b) The final product is a concentrated sludge that arises to secondary pollution and disposal issue after the treatment process.
Adsorption	(a) No hazardous intermediate product will be produced in the adsorption process.	(a) The process involves phase transfer of dyes, resulting in the production of secondary waste and post-treatment is required for the proper disposal. (b) Concentrated sludge is produced, and higher running cost is required.
Biodegradation	(a) This treatment technique is relatively inexpensive, low running cost and the final products is non-toxic.	(a) The treatment process is less flexible in design and operation, and requires a larger land area and a longer time for the degradation and fermentation process, which making it incapable of decolourize the dyes in a continuous system.
Fenton process	(a) Highly effective for the decolourization of soluble and insoluble dyes. (b) The reduction of COD and TOC is achieved instead of only colour removed.	(a) The process is usually effective within narrow pH range of less than 3.5. (b) Longer time is required for the reaction and higher sludge is generated after the treatment process.

2.2 Photocatalysis

2.2.1 Definition and historical introduction

Over the past decades, most of the published photocatalysis research was originated from the top 11 nations, including China, Japan, United States, South Korea, India, Germany, Italy, France, Spain, United Kingdom and Iran as summarized in Figure 2.2. Amongst all, although Japan and United States are recognized as the traditional photocatalysis powerhouse, but the research output from China has dominated this field followed by India until present. Today, South Korea has also experienced substantial growth on the research pertaining to photocatalysis (Teoh *et al.*, 2012). Figure 2.3 shows the historical timeline of photocatalysis from 1910s to 2010s. The details of the historical activities are summarized in Table B1 (Appendix B).

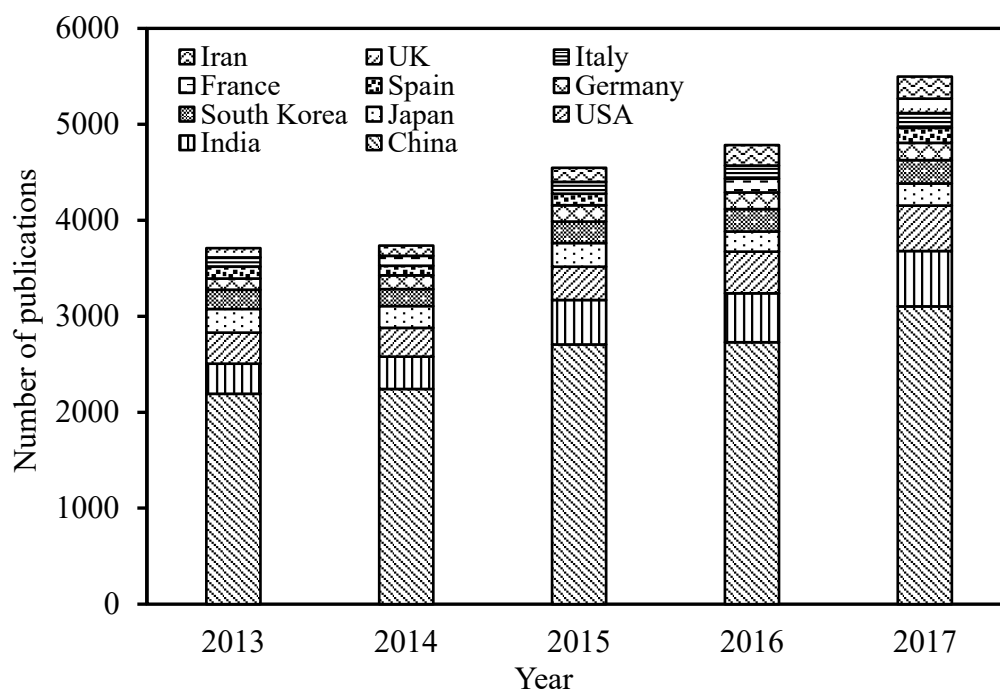


Figure 2.2: Number of publications related to photocatalysis from 2013-2017 in different countries.

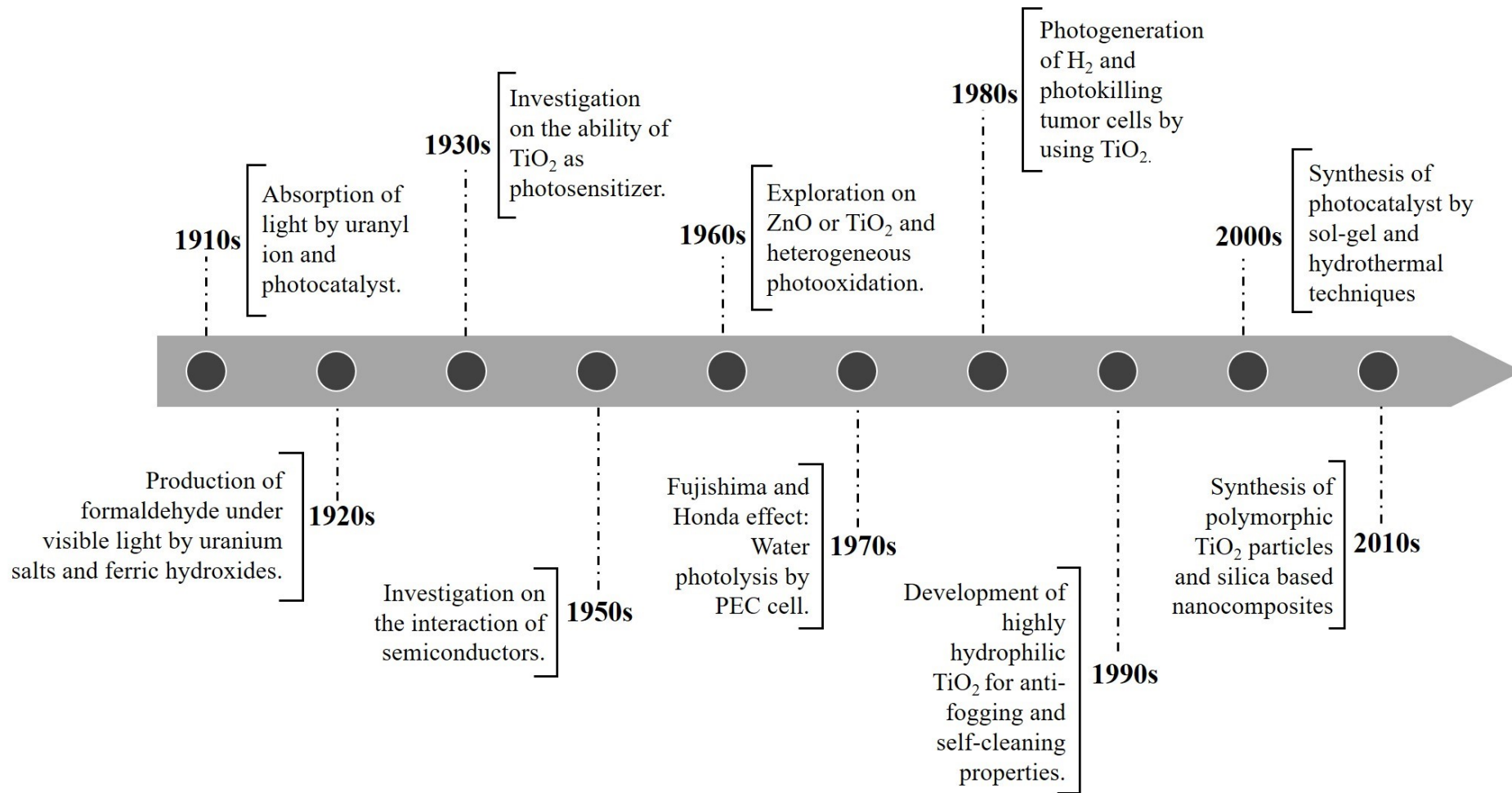


Figure 2.3: Historical timeline of photocatalysis from 1910s to 2010s.

Historically, as early as in 1910s, the term “photocatalysis” has been introduced in most of the scientific communication. The term is originated from Greek, which composes of two parts: “photo” (*phos*) and “catalysis” (*katalyo*). In English, the prefix “*phos*” means light while “*katalyo*” gives the meaning of breaking apart or decomposing (Kondarides, 2005). However, it can be defined simply as the acceleration of a photoreaction with the presence of a catalyst. In a proper scientific definition, photocatalysis is termed as “changes in the rate of chemical reaction with the presence of photocatalysts via regeneration of electron-hole pairs accompanied by the absorption of photon energy under the exposure of UV or visible light” (Escobedo Salas, 2013). Based on this concept, photocatalysis has been incorporated into several studies by the recognized researchers in Germany and France (Coronado *et al.*, 2013).

In 1910s, scientists began to imply the absorption of light by uranyl ion and photocatalyst, a material that accelerates the chemical reaction without changing itself after the absorption of a photon (Oka *et al.*, 2008). In the late 1920s, Keidel and co-workers has recognized the influence of rutile in the light-induced fabrics and paints (Coronado, 2013). Subsequently, the first study on the ability of TiO₂ as the semiconducting photocatalyst for the degradation of dyes was introduced by the research team of Goodeve and Kitchener in the late 1930s (Simonsen, 2014). During these investigations, the basic principles of heterogeneous photocatalysis have been discovered. It is a photocatalytic process with the presence of metal oxides, in the different phase from the reactant” (Escobedo Salas, 2013).

In heterogeneous photocatalysis, discoloration of organic solvents was found by photooxidation, in which active oxygen species was produced on the surface of TiO₂ after the absorption of UV light. However, the interest on the ability of semiconducting photocatalyst was nearly faded in the next decades, due to the absence

of practical application and the drawback of its applications for inorganic chemicals (Serpone *et al.*, 2012). Extending to the late 1950s, a relevant study on semiconductors and its photocatalytic mechanism was again introduced by Terenin (Lisachenko, 2018). Following the research direction, this aforementioned study has induced a growing interest on the potential utilization of different kind of metal oxides such as TiO₂ and ZnO for the photodegradation of organic chemicals in the 1960s. Although the evaluation of heterogeneous photocatalysis has been adopted before 1970s, the application of photocatalysis was extensively promoted by the appreciable discovery, known as “Fujishima and Honda effect”, a pioneering study induced by two Japanese researchers in the early 1970s.

Coinciding with this economically convulse time, a landmark paper about the photolysis of water into hydrogen and oxygen by using a rutile TiO₂ in the photoelectrochemical (PEC) cell has been recognized by the research group of Fujishima and Honda (Walter *et al.*, 2010). Accordingly, the PEC system involved photocatalytic water splitting process from the evolution of O₂ at a single crystal rutile TiO₂ electrode, and the evolution of H₂ at the inert platinum (Pt) counter-electrode via an electrical load during the irradiation of UV light. The schematic diagram of the PEC cell is presented in Figure 2.4. This developed innovative technology had opened up a new possibility for the generation of sustainable solar hydrogen as an alternative fuel source. After that, researches related to the heterogeneous photocatalysis have increased progressively, and the rapid development of functional photocatalysis was advocated for the environmental remediation and anti-bacterial properties in the early 1980s (Teoh *et al.*, 2012). Within this framework, several investigations have been carried out to evaluate the applications for the reduction of nitrogen, and the ability of TiO₂ on photokilling microbes (Schrauzer, 2011; Yadav *et al.*, 2016).

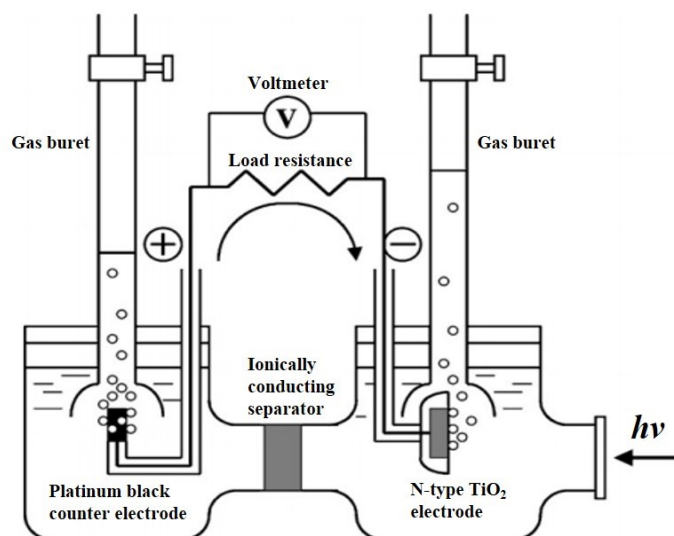


Figure 2.4: Schematic diagram of the electrochemical photocell (Hashimoto *et al.*, 2005).

In 1990s, extensive fundamental knowledge on photochemistry and photo-physics was established, including the understanding of photoinduced charge transfer across the surfaces of photocatalyst and radical chemistry of TiO_2 (Williams *et al.*, 2008). The mechanisms of organic photocatalytic oxidation had also become the focal points of most of the research in corresponding to the interest in water and air pollution abatement. In 2000s, a developing interest in heterogeneous photocatalysis has been heightened exclusively, and a significant amount of publications in the field comprises of photocatalyst synthesis and the photo-mediated utilizations. Since 2010s, photocatalysis has appeared to be a new emerging “advanced oxidative process (AOP)”, with more than 1500 publications relevant to this field and the number of publications keep increasing, with about 5500 articles have been published till 2017 (Figure 2.2). Nowadays, of the latest progress in photocatalysis, major advances have been driven by the integration of nanotechnology and materials science in designing an innovative, effective photocatalyst, and a functional photocatalytic system.

2.2.2 Basic concept and mechanism of photocatalysis

Heterogeneous photocatalysis is a part of AOPs that have been proven to be a promising green technology for organic synthesis, water splitting, photoreduction, hydrogen transfer, isotopic exchange, metal deposition, water purification, and gaseous pollutant detoxification (Carp *et al.*, 2004). The basic photophysical and photochemical principle pertaining to photocatalysis have been established and literately documented (Dung *et al.*, 2005). Basically, the heterogeneous photocatalytic reaction involves both oxidation and reduction in the presence of semiconductor photocatalyst, potential oxidizing agents such as oxygen or air and a light source (Ahmed *et al.*, 2011). Figure 2.5 depicts the basic pathway of the heterogeneous photocatalysis process of water pollutants on the surface of TiO_2 .

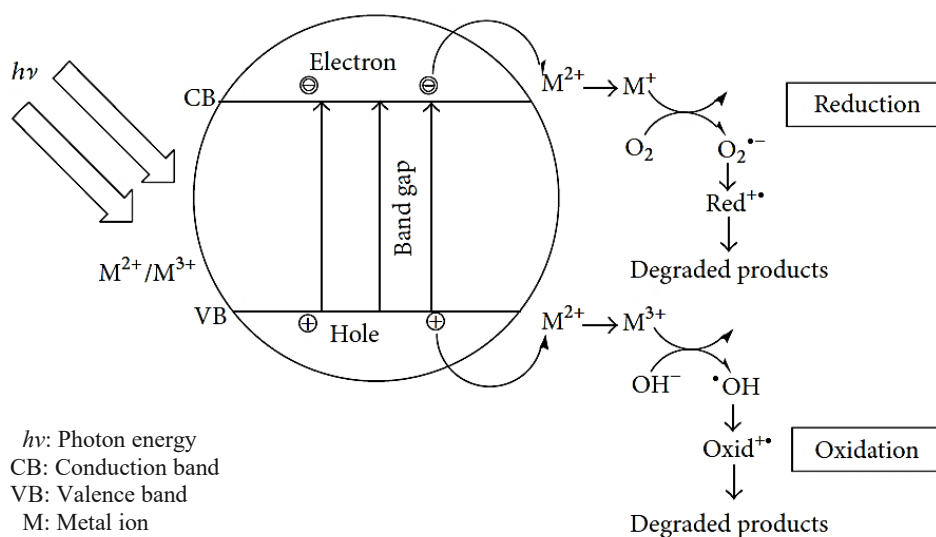
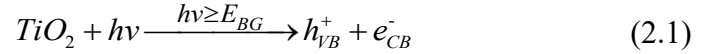


Figure 2.5: Schematic diagram of basic photocatalytic processes over photon activated semiconductor photocatalyst (Mahlambi *et al.*, 2015).

Under the exposure to UV light with wavelength, photoexcitation of the catalyst would be induced, and the predominant reactions representing the key steps in the photocatalytic reactions are listed as:

(a) Photoexcitation:



(b) Ionization of water:



(c) Oxidation and reduction:



(d) Protonation of superoxide:



(e) Recombination of electron-hole pairs:



When the absorbed photon energy ($h\nu$) equals or greater than the band gap energy (ΔE) of metal oxide, the photoexcited electron in valence band (VB) is promoted to the empty conduction band (CB). This absorption of light would lead to